Inorganic Chemistry

Article

pubs.acs.org/IC

$Na_{1.515}EuGeS_4$, A Three-Dimensional Crystalline Assembly of Empty Nanotubules Constructed with Europium(II/III) Mixed Valence Ions

Amitava Choudhury,[†,‡] Fernande Grandjean,[‡] Gary J. Long,*[,‡] and Peter K. Dorhout*[,†,§]

[†]Department of Chemistry, Colorado State University, Fort Collins, Colorado 80523, United States

[‡]Department of Chemistry, Missouri University of Science and Technology, University of Missouri, Rolla, Missouri 65409-0010, United States

Supporting Information

ABSTRACT: A new compound, $Na_{1.515}EuGeS_4$, has been synthesized at 750 °C from a reaction of elemental europium, germanium, and sulfur and Na_2S. The compound crystallizes in the trigonal system with $Z = 18$ and the $R3c$ space group with $a = 23.322(3)$ Å, $c = 6.838(1)$ Å, and $V = 3221.2(9)$ Å^3. $Na_{1.515}EuGeS_4$, which is isostructural with $Na_2EuSiSe_4$, contains quasi-infinite nanoscale $_\infty[EuGeS_4]^{2-}$ tubules that are held together by sodium cations through electrostatic interactions. The tubules consist of a complex network of monoface-capped EuS_7 trigonal prisms and GeS_4 tetrahedra. The most striking structural feature of $Na_{1.515}EuGeS_4$ is the absence of sodium cations inside the tubules, an absence that is balanced by the presence of mixed valence europium(II/III) ions. This mixed valence is confirmed by europium-151 Mössbauer spectroscopy, which indicates discrete mixed-valence europium ions at least up to 295 K. The stoichiometry has been determined by a fit of $\chi_M T$ measured between 20 and 300 K with a combination of europium(II) ions, with a Curie constant of 7.877 emu K/mol, and europium(III) ions whose contribution to $\chi_M T$ has been fit by using the Van Vleck expression for its molar susceptibility. The best fit corresponds to 51.5% of europium(II), 48.5% of europium(III), a stoichiometry of $Na_{1.515(5)}EuGeS_4$, and a splitting, E, between the $J = 0$ and the first excited $J = 1$ state of europium(III) of 360(6) cm^{-1}. The field dependence of the 1.8 K magnetization is in perfect agreement with a $S = 7/2$ Brillouin function with $g = 2.00$ and yields a saturation magnetization of 7 Nβ at 5 T.

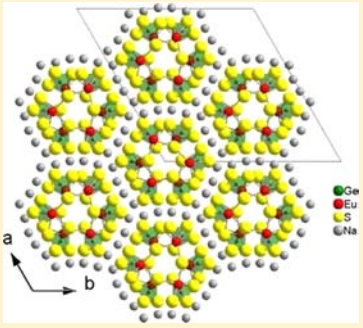

INTRODUCTION

Low dimensional solid-state materials have long been of interest to the physics, chemistry, and materials communities and, more recently, the interest in layered transition metal chalcogenides and oxy-pnictides has expanded due to the discovery of superconductivity in some of these materials.[1,2]

Solid state low-dimensionality often arises because covalent connectivity extends only in one or two directions leading to one-dimensional chains or two-dimensional layers, chains or layers that are then held together by van der Waals or electrostatic forces. Often alkali metal cations reside between the one- or two-dimensional chains or layers of these solids. Both MoS_2 and WS_2 are the classic examples in which a two-dimensional layered solid is held together by van der Waals forces and, as a consequence, they are very good catalysts for several processes.[3] Interestingly, the layers of MoS_2 and WS_2 and similar materials can be folded onto themselves to form a tubular or closed shell geometry and are then referred to as inorganic nanotubes or inorganic fullerenes, respectively.[4] These inorganic nanotubes or fullerenes form a new class of low-dimensional materials that exist independently and often exhibit unique properties.[5]

Recently, a limited number of a fascinating class of compounds has been reported whose crystal structures contain nanoscale features such as nanotubules or nanospheres.[6−13] These nanoscale features are different from the so-called inorganic "nanotubes or nanoparticles" because they do not have any independent existence as a stand-alone nanotube or nanoparticle. Rather, they are always bound through a periodic arrangement into a three-dimensional crystalline assembly and held together by electrostatic forces. For example, nanotubules have been observed both in many oxide based materials, such as $Na_2V_3O_7$,[7] $(C_4H_{12}N)_{14}[(UO_2)_{10}(SeO_4)_{17}(H_2O)]$,[8] $K_5[(UO_2)_3(SeO_4)_5](NO_3)(H_2O)_{3.5}$,[9] and $Cs_{3.62}H_{0.38}[(UO_2)_4\{C_6H_4(PO_2OH)_2\}_3\{C_6H_4(PO_3)_2\}F_2]$,[10] and in chalcogenides, such as $SbPS_4$ and $Na_2EuSiSe_4$.[11,12] Nanospheres have been observed in many actinyl oxides and peroxides with exotic structures.[13]

Both nanotubules and nanospheres are emerging as an attractive class of materials because of the possibility of forming nanotubes or nanoparticles with a uniform diameter, which is an important goal in current nanomaterials research. However, it is still a challenge to overcome the attractive forces of the crystal lattice and thus isolate the nanotubules or particles from each other, thereby leading to a stand-alone existence.

We have previously reported a europium(II) selenosilicate, $Na_2EuSiSe_4$, with a nanotubular structure in which the tubules were partially filled with sodium cations.[12] Herein, we report the synthesis, structure, magnetic, and europium-151 Mössba-

Received: August 6, 2012
Published: October 16, 2012

   dx.doi.org/10.1021/ic301724v | *Inorg. Chem.* 2012, 51, 11779−11786

uer spectral properties of a new tubular mixed-valence europium(II/III) thio-germanate, $Na_{1.515}EuGeS_4$, **1**, a compound that has an empty channel and is isostructural with $Na_2EuSiSe_4$.

EXPERIMENTAL SECTION

Synthesis. $Na_{1.515}EuGeS_4$ has been prepared as the result of an attempt to synthesize Na_2EuGeS_4, the isostructural tubular analogue of $Na_2EuSiSe_4$. In an N_2-filled glovebox, a stoichiometric mixture of elemental sulfur, germanium, europium, and Na_2S, were placed in a fused-silica ampule. The sulfur (Johnson–Mathey, 99.999%), germanium (Alfa Aesar, 99.9% powder), europium (Alfa Aesar, 99.9% powder), and Na_2S (Cerac, −60 mesh) were used as received. The ampules were flame-sealed under vacuum and placed in a temperature-controlled furnace. The furnace temperature was increased to 750 °C at a rate of 35 °C/h, and then held constant at 750 °C for 150 h. The furnace temperature was then slowly reduced to ambient temperature at a rate of 5 °C/h. The cooled ampule was opened in air and the reaction product contained bundles of dark red long hexagonal rods; there was also a small amount of yellowish deposit at the cold end of the ampule.

Single-crystal energy dispersive X-ray analyses indicated that the actual composition of the reaction product was deficient in sodium cations and had a stoichiometry of Na_xEuGeS_4 where x was 1.5 to 1.6. As will be discussed below, subsequent magnetic measurements, which are the most accurate method for determining x, lead to a stoichiometry with $x = 1.515(5)$, a stoichiometry that is consistent with both the single-crystal X-ray structural and europium-151 Mössbauer spectral analysis presented below. Consequently, the best formulation of the reaction product, see below, is $Na_{1.515(5)}Eu(II)_{0.515(5)}Eu(III)_{0.485(5)}GeS_4$; herein this product will be referred to as $Na_{1.515}EuGeS_4$, **1**. Subsequent synthesis of **1** with the exact stoichiometric amounts of starting materials, in the absence of the Na_2S flux, led to the same product, but with an absence of any yellowish deposit at the cold end of the reaction ampule.

Single Crystal X-ray Diffraction. Intensity data sets for **1** were collected on a Bruker Smart CCD diffractometer. The data were integrated with SAINT,[14] and the program HABITUS[15] was used for the absorption correction. The structure was solved by direct methods using SHELXS-97[16] and difference Fourier syntheses. Full-matrix least-squares refinement against $|F^2|$ was carried out by using the SHELXTL-PLUS[16] suite of programs. On the basis of systematic absences, the $R3c$ space group was chosen for **1**, a choice that indicates that **1** is isostructural with its seleno-silicate analogue, $Na_2EuSiSe_4$. The europium, germanium, and the four sulfur ions were easily located on the 18*b* crystallographic sites.

Subsequent refinements identified two sodium cations at 2.791(2) and 2.955(3) Å from S1 and S2, respectively. These ions were designated as Na1 and Na2 and refined isotropically, a refinement that indicated a large isotropic thermal parameter, U_{iso}, of 0.136(4) Å^2 that may signify a partial occupancy of the Na2 site. In subsequent refinements, when the occupancy of Na2 was varied, it refined to a value of 0.522(6) and also decreased U_{iso}, to 0.056(2) Å^2. However, based on the magnetic results mentioned above and discussed below, the occupancy of Na2 was fixed to 0.515, which corresponds to the $Na_{1.515}EuGeS_4$ composition. The resulting refinement with this occupancy constraint was virtually as good as the unconstrained fit. The last cycles of refinement for **1** included anisotropic thermal parameter refinements for all the ions. Details of the final refinement and the crystallographic parameters for **1** are given in Table 1. The final coordinates and important interionic distances and angles for **1** are given in Tables 2 and 3, respectively.

Physical Property Measurements. Diffuse reflectance spectra were collected on a Varian Cary 500 UV–vis-NIR spectrophotometer equipped with a Praying Mantis accessory. A polyTeflon standard was used as a reference. The Kubelka–Munk theory was used to obtain the optical absorbance in terms of α/S, the unitless ratio of the absorption coefficient to the scattering coefficient.[17]

Table 1. Crystal Data and Structure Refinement for $Na_{1.515}EuGeS_4$, 1

chemical stoichiometry	$Na_{1.515}EuGeS_4$
formula weight, g/mol	387.64
space group	$R3c$ (no. 161)
temperature, K	293
wavelength, Å	0.71073
a, Å	23.322(3)
c, Å	6.8385(16)
volume, Å^3	3221.2(9)
Z	18
ρ_{calc}, Mgm^{-3}	3.597
μ, mm^{-1}	14.017
R_1 $[I > 2\sigma(F^2)]^a$	0.0525
wR_2 (F^2) (all data)^b	0.1127

$^aR_1 = \Sigma ||F_o| - |F_c||/\Sigma|F_o|$. $^bwR_2 = \{\Sigma [w(F_o^2 - F_c^2)^2]/\Sigma [w(F_o^2)^2]\}^{1/2}$, $w = 1/[\sigma^2(F_o)^2 + (aP)^2 + bP]$, where $P = [F_o^2 + 2F_c^2]/3$; $a = 0.0563$ and $b = 0.000$.

The magnetic properties were measured with a Quantum Design MPMS XL superconducting quantum interference magnetometer. The magnetic susceptibility of a collection of crushed single crystals of **1** was measured, after cooling either to 4.8 or 1.8 K in a 10 Oe applied field, upon warming to 300 K in a dc applied field of 0.5 T. The former measurements were obtained with the standard transport method, whereas the latter were obtained with the reciprocating sample option; the results were identical within experimental error. The magnetic susceptibility of **1** was also measured, after zero-field cooling to 1.8 K, upon warming from 1.8 to 30 K in a 10 Oe dc applied field and, subsequently, upon field-cooling from 30 to 1.8 K in a 10 Oe dc field. The molar magnetic susceptibility was corrected for the intrinsic diamagnetism of the constituents of **1** by subtracting −0.000098 emu/mol, a correction that was obtained from Pascal's constants.[18]

The isothermal magnetization was measured at 1.8 K between 0 and 5 T; the slope of the magnetization at fields between 0 and 0.25 T yielded a molar magnetic susceptibility that was consistent with that observed at 1.8 K and 10 Oe.

The europium-151 Mössbauer spectra were measured at 85 and 295 K on a constant-acceleration Wissel spectrometer which utilized a SmF_3 source. The isomer shifts are reported relative to EuF_3 at room temperature with an estimated error of ±0.05 mm/s. The absorber contained 140 mg/cm^2 of powdered sample mixed with boron nitride. Unfortunately, because of the small amount of europium in the sample, three and eight days were required to obtain the spectra at 85 and 295 K, respectively. Because of the long times required to obtain the spectra, no lower temperature spectra were measured. The velocity scale was calibrated at room temperature with a cobalt-57 source and an α-iron absorber.

RESULTS AND DISCUSSION

X-ray Structure. The structure of **1** consists of nanotubules of $[EuGeS_4]^{2-}$ packed hexagonally and held together by sodium cations, see Figure 1. The inner and outer diameters of the tubules, calculated from the circum-circle of equilateral triangles formed by the three inner and outermost sulfur ions, are 4.47(2) and 11.52(1) Å, respectively.

The asymmetric unit of **1** contains eight crystallographically distinct sites comprising four sulfur, one germanium, one europium, and two sodium cations, Na1 and Na2, with partial occupancy of the Na2 site. In contrast to the isostructural $Na_2EuSiSe_4$ compound, $Na_{1.515}EuGeS_4$, **1**, does not have a third sodium cation site, a site that is located on a 3-fold rotation symmetry axis in the center of the channels, in $Na_2EuSiSe_4$.[12] The absence of this sodium cation in **1** has necessitated a partial oxidation of europium(II) to europium(III) in order to

dx.doi.org/10.1021/ic301724v | Inorg. Chem. 2012, 51, 11779–11786

Table 2. Positional Coordinates (× 10^4) and Equivalent Isotropic Displacement Parameters (× 10^3) for $Na_{1.515}EuGeS_4$, 1

site	Wyckoff	x	y	z	U_{eq},[a] Å^2	occupancy
Ge	18*b*	5187(1)	6647(1)	4166(3)	17(1)	1
Eu	18*b*	4781(1)	6748(1)	9163(1)	18(1)	1
S(1)	18*b*	4980(3)	5865(2)	6339(6)	36(1)	1
S(2)	18*b*	5700(2)	7570(2)	5910(5)	22(1)	1
S(3)	18*b*	4263(2)	6610(2)	3184(6)	26(1)	1
S(4)	18*b*	5794(2)	6648(2)	1656(6)	20(1)	1
Na(1)	18*b*	4592(4)	4632(3)	4663(10)	33(2)	1
Na(2)	18*b*	6470(8)	7035(9)	7820(30)	47(3)	0.515

[a] U_{eq} is defined as one-third of the trace of the orthogonalized U_{ij} tensor.

Table 3. Selected Interatomic Bond Distances and Angles for the Coordination Polyhedra of $Na_{1.515}EuGeS_4$, 1[a]

moiety	distances (Å)	moiety	distances (Å)
Ge(1)−S(1)	2.212(5)	Na(2)−S(1)	3.33(2)
Ge(1)−S(2)	2.216(4)	Na(2)−S(2)	2.945(15)
Ge(1)−S(3)	2.217(5)	Na(2)−S(4)$^{\#7}$	2.870(15)
Ge(1)−S(4)	2.224(4)	Na(2)−S(4)$^{\#4}$	2.962(15)
		Na(2)−S(1)$^{\#7}$	3.099(19)
Eu(1)−S(3)$^{\#4}$	2.955(5)	Na(2)−S(4)$^{\#12}$	3.163(18)
Eu(1)−S(3)$^{\#5}$	2.978(5)	moiety	angle, deg
Eu(1)−S(3)$^{\#6}$	2.985(5)	S(1)−Ge(1)−S(2)	103.23(18)
Eu(1)−S(4)$^{\#4}$	3.019(4)	S(1)−Ge(1)−S(3)	111.4(2)
Eu(1)−S(2)	3.018(4)	S(2)−Ge(1)−S(3)	104.12(18)
Eu(1)−S(1)	3.026(5)	S(1)−Ge(1)−S(4)	113.23(19)
Eu(1)−S(2)$^{\#6}$	3.082(5)	S(2)−Ge(1)−S(4)	112.32(18)
		S(3)−Ge(1)−S(4)	111.90(18)
Na(1)−S(1)	2.789(9)		
Na(1)−S(1)$^{\#9}$	2.844(9)		
Na(1)−S(2)$^{\#11}$	2.858(8)		
Na(1)−S(4)$^{\#11}$	2.878(9)		
Na(1)−S(4)$^{\#5}$	2.887(8)		
Na(1)−S(2)$^{\#1}$	2.934(8)		

[a] Symmetry transformations used to generate equivalent atoms: $^{\#1}$ $-y + 4/3, x - y + 2/3, z - 1/3$; $^{\#4}$ $x, y, z + 1$; $^{\#5}$ $-y + 1, -x + 1, z + 1/2$; $^{\#6}$ $x, x - y + 1, z + 1/2$; $^{\#7}$ $-x + y + 2/3, -x + 4/3, z + 1/3$; $^{\#9}$ $-y + 1, -x + 1, z - 1/2$; $^{\#11}$ $-x + y + 1/3, y - 1/3, z + 1/6$; $^{\#12}$ $-y + 4/3, x - y + 2/3, z + 2/3$.

maintain charge balance if the formal oxidation state of germanium is assumed to be +4 and that of sulfur is assumed to be −2. Thus **1**, as is shown below, is a class-2 mixed valence compound[19] containing europium(II) and europium(III) ions on the same crystallographic site.

The Ge−S distances in the GeS_4 tetrahedra are in the range of 2.212(5) to 2.225(4) Å with an average distance of 2.217(5) Å. The europium(II/III) ions have a distorted monofaced capped trigonal prismatic coordination geometry, where the trigonal prism is somewhat distorted, and are coordinated to seven sulfur ions with the prismatic Eu−S distances ranging from 2.955(5) to 3.019(4) Å with an average distance of 2.997(5) Å; the face capping Eu−S2 distance is 3.082(5) Å, see Figure 2a.

The sodium cations are surrounded by six sulfur ions, where Na1 and Na2 adopt a regular and distorted octahedral coordination geometry, respectively, see Figure 2b. The Na1−S distances are in the range of 2.791(8) to 2.932(8) Å with an average distance of 2.864(8) Å, whereas the Na2−S distances are in the range of 2.873(5) to 3.33(2) Å with an average distance of 3.062(5) Å. As noted above, because there is only one europium crystallographic site, both europium(II) and europium(III) are located on the same site and are crystallographically equivalent. The presence of mixed valence europium ions is also reflected in the bond valence sum[20] of 2.23(3) Å. The Eu−S bond distances are also in good agreement with those previously reported in mixed valence europium-sulfide compounds in which europium(II) and europium(III) ions are also located on a crystallographically unique site.[21,22]

In the above formulation of **1** as $Na_{1.515(5)}Eu(II)_{0.515(5)}Eu(III)_{0.485(5)}GeS_4$ it has been assumed that the elements are present in the +1, +2, +3, +4, and −2 formal valence states, respectively. It seems likely that the sodium cation must be +1 and the Mössbauer spectral isomer shifts indicate that the formal valence states of the europium cations must be +2 and +3 or very close to these values. But it is quite possible that some of the sulfur may be present as $(S_2)^{2-}$ dimeric dianions in **1**, a presence which would lower the formal valence state of the germanium cation from +4 to a smaller value depending upon the amount of sulfur present as $(S_2)^{2-}$ dimeric dianions. However, if $(S_2)^{2-}$ dimeric dianions are present in **1**, one would expect a rather short S−S bond distance, but the crystal structure of **1** indicates that the S−S distances range from 3.470(6) Å for S(1)−S(2) to 3.788(8) Å for S(2)−S(3), distances that are not particularly short; indeed these distances are close to the 3.60 Å sum of the van der Waals radii of two sulfurs. The S−S distances are in the range of 2.0 to 2.2 Å in compounds with an unequivocal presence of an $(S_2)^{2-}$ bond. For example, in $Cs_4(S_2)_2(GeS_2)$ and LaS_2, the S−S distances[23,24] in the $(S_2)^{2-}$ dimeric dianions are 2.077(2) and 2.112(3) Å, respectively. Thus it seems most likely that sulfur is present in the formal −2 valence state in **1**.

As might be expected, the thermal factors of the sulfur ions in **1** are large because of their bonding to both the mixed valence europium(II/III) site and to the partially occupied Na2 site. The equivalent isotropic thermal factors for the germanium and europium sites are 0.017(1) and 0.018(1) Å^2, respectively, whereas the S1 to S4 values are 0.036(1), 0.022(1), 0.026(1), and 0.020(1) Å^2, respectively, with an average value of 0.026(1) Å^2. Further, the germanium and europium site thermal factors are close to isotropic whereas those of the sulfur sites are quite anisotropic.

There is no indication of any unit cell superstructure that could result from charge ordering of the europium cations in the room temperature X-ray diffraction results. Hence, at least at room temperature, the structure of **1** is best described as having a random distribution of the europium(II) and europium(III) cations on the unique europium 18*b* crystallographic site.

dx.doi.org/10.1021/ic301724v | *Inorg. Chem.* 2012, 51, 11779−11786

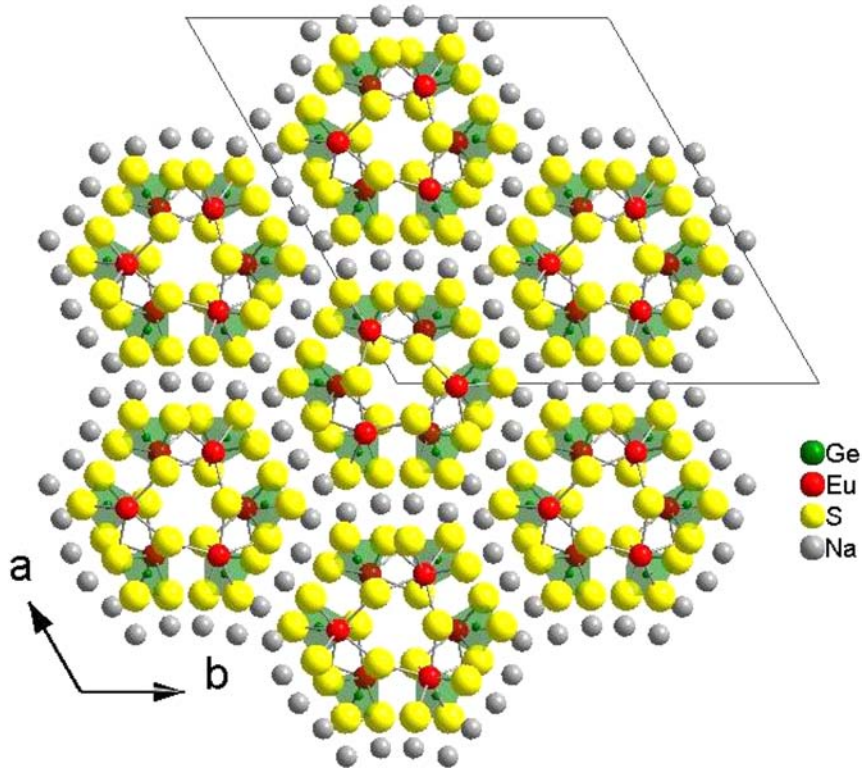

Figure 1. Structure of $Na_{1.515}EuGeS_4$, **1**, viewed down the *c*-axis. The GeS_4 tetrahedra are shown in green.

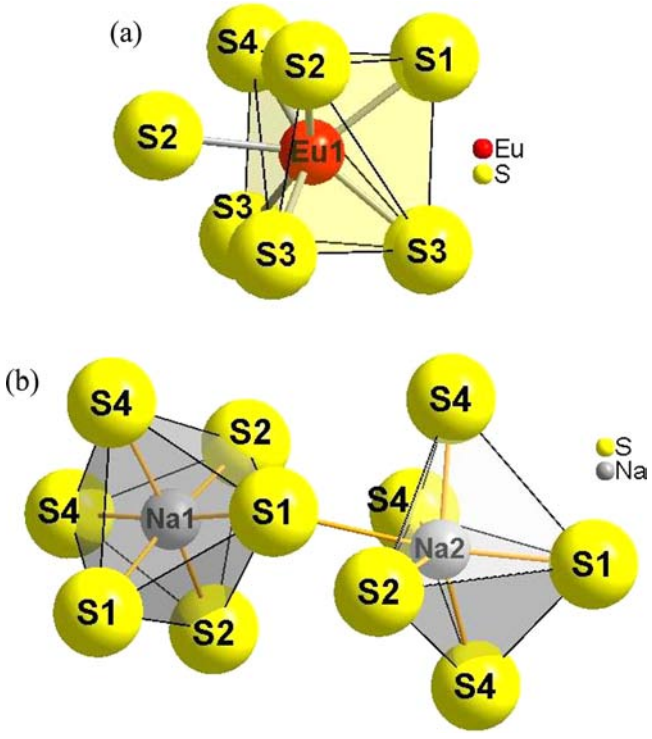

Figure 2. Polyhedral representation of the coordination environment of the europium ion, a, and the coordination environment at the two crystallographically independent sodium cations, b, in $Na_{1.515}EuGeS_4$, **1**.

Because compound **1** is isostructural with $Na_2EuSiSe_4$,[12] no further detailed discussion of its structure is required herein. One may recall from this earlier work that the structure of $Na_2EuSiSe_4$ may be described in terms of $_\infty[EuGeS_4]^{2-}$ tubules oriented along the *c*-axis in which three EuS_7 polyhedra are linked through their corners to form an equilateral triangle or a cyclic trimer, trimers that are then stacked one above another in a staggered configuration and condensed together through their edges to form a tubule. The germanium ions fill the tetrahedral holes created by the Eu−S network. The channels of the tubules are empty in **1**, whereas they were filled with sodium cations in the isostructural $Na_2EuSiSe_4$ compound. A scan of the electron density map did not reveal any noteworthy electron density within the tubules that could suggest even a partial occupation by sodium cations in sites that were occupied by sodium cations in $Na_2EuSiSe_4$. The anionic tubules of $_\infty[EuGeS_4]^{2-}$ are held together by the Na1 and Na2 cations that reside in the intertubular space and, as a consequence, electrostatic interactions are responsible for the cohesion between the tubules and an organized three-dimensional assembly of the tubules is formed. The $Na1S_6$ and $Na2S_6$ octahedra form edge-shared and face-shared one-dimensional chains along the *c*-axis, respectively.

Europium-151 Mössbauer Spectra. The europium-151 Mössbauer spectra of $Na_{1.515}EuGeS_4$, **1**, obtained at 85 and 295 K are shown in Figure 3; both exhibit two well separated but rather broad spectral components. Although the resolution of europium-151 Mössbauer spectroscopy is somewhat limited by its typical line width of ca. 2.3 mm/s, it does have the advantage of yielding quite different isomer shifts for europium(II) and europium(III) ions, at least when they are present in discrete valence states as is the case for **1**.

Although the two spectral components observed in the spectra of **1** can each be well fit with a single Lorentzian line, the resulting line widths are rather larger than expected and, further, the coordination environment about the europium ions is not cubic. Thus, both spectral components have been fit with

dx.doi.org/10.1021/ic301724v | *Inorg. Chem.* 2012, 51, 11779−11786

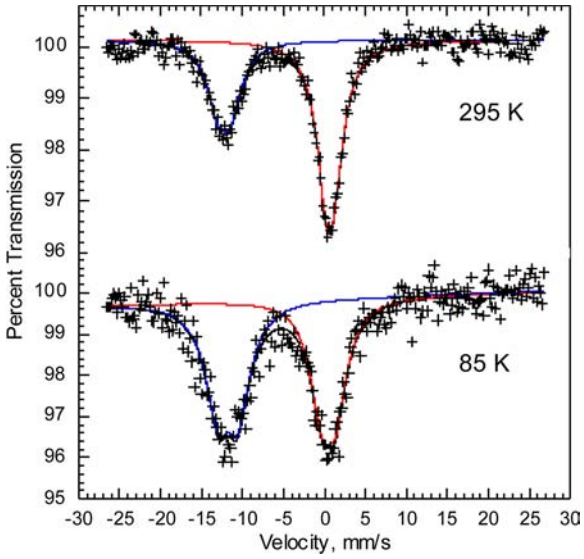

Figure 3. Europium-151 Mössbauer spectra of $Na_{1.515}EuGeS_4$, **1**, obtained at the indicated temperatures. The europium(II) spectral component is shown in blue and the europium(III) spectral component is shown in red.

an isomer shift and a quadrupole interaction, eQ_gV_{zz}, for the $I = 5/2$ nuclear ground state, where Q_g is the ground state nuclear quadrupole moment; eQ_eV_{zz} for the $I = 7/2$ nuclear excited state, where Q_e is the excited state nuclear quadrupole moment, has been constrained such that $Q_e = 1.34\ Q_g$. Preliminary fits indicated that the asymmetry parameter, η, was one within error limits, as would be expected[25] for the observed symmetric spectral absorptions and, as a consequence, this parameter was constrained to $\eta = 1$ in the final fits. The results of these fits, which involve the variation of the isomer shift, δ, the quadrupole interaction, eQ_gV_{zz}, the line width, Γ, the spectral absorption area, and the spectral absorption baseline, are shown as the solid lines in Figure 3; the resulting parameters are given in Table 4.

At 85 K, the area ratio of the europium(II) to europium(III) spectral components is 1.12(3), a value that is in very good agreement with the more accurate ratio of 1.06(2) obtained from the magnetic analysis discussed below. The difference is most likely an indication that the recoil-free fraction, f, of the two ions is slightly different even at 85 K. Further, at 295 K this ratio decreases to 0.57(3) because the recoil-free fraction, f, of the europium(II) ion decreases, as expected, more rapidly with warming than does that of the europium(III) ion.

The observed 85 and 295 K isomer shifts of −11.79(6) and −12.13(6) mm/s, respectively, are characteristic[25] of europium-(II) and, although small, their decrease with increasing temperature is expected because of the second-order Doppler shift.[26] Further, the observed 85 and 295 K isomer shifts of 0.50(5) and 0.68(3) mm/s, respectively, are characteristic[25] of europium(III), but the small increase upon warming is, although small, unexpected and may indicate that the true errors may be twice the statistical errors given in Table 4.

The europium(II) isomer shift of −11.79(6) mm/s observed for **1** at 85 K is in excellent agreement with both the −11.56 mm/s isomer shift reported[27] for EuS at 4.2 K and the ca. −11.7 mm/s reported[28] for the europium(II) ion in Eu_3S_4 at 77 K. The reported[28] value of ca. 0.1 mm/s at 77 K for the europium(III) is similar to the 0.50(5) mm/s observed for **1** at 85 K. It is interesting to note that above 160 K Eu_3S_4 is valence delocalized,[28] whereas in **1** the europium(II) and europium(III) valencies remain localized at least up to 295 K, confirming that **1** is a class-2 mixed valence compound.

Samuel and Delgass[29] have shown that hybridization of the 4*f* electrons with the 6*s* electrons will affect the europium-151 isomer shift. Specifically, the $4f^7 6s$ electronic configuration has an isomer shift that is ca. 6 mm/s greater than that of the free-ion europium(II) $4f^7$ electronic configuration. Further, there is a positive difference[29] of ca. 10 mm/s between the isomer shifts of the $4f^7$ and $4f^6$ electronic configurations. The positive difference of 1.4 mm/s between the isomer shift of −12.13(6) mm/s at 295 K measured herein for **1** and the isomer shift of −13.5 mm/s isomer shift observed[29] at 295 K for EuF_2, represents a gain of 0.23 6*s* electrons or a loss of 0.14 4*f* electrons. Consequently, we may assume that in **1**, the average electronic configuration of the europium(II) ion is between $4f^7 6s^{0.23}$ and $4f^{6.86}$, configurations that are consistent with a formal divalent oxidation state.

At both 85 and 295 K, the quadrupole interactions, eQ_gV_{zz}, are small as would be expected[25] for the europium ion coordination environment. Further, for both oxidation states the quadrupole interaction decreases somewhat upon warming.

Magnetic Susceptibility. The temperature dependence of the molar magnetic susceptibility, χ_M, of $Na_{1.515}EuGeS_4$, **1**, has been measured upon warming from 4.8 to 300 K in a 0.5 T dc applied magnetic field after cooling to 4.8 K in a 10 Oe field.

A fit of $\chi_M T$ between 20 and 300 K is shown in the main portion of Figure 4. The $\chi_M T$ observed between 4.8 and 20 K has not been fit because of the apparent onset of long-range magnetic ordering below ca. 12 K. An analogous plot of χ_M is shown in Figure S1 of the Supporting Information, SI. Because of the presence of both europium(II) and europium(III) in **1**, this fit has used the expression,

$$\chi_M T = a\chi_M^{II} T + (1 - a)\chi_M^{III} T + N\alpha T$$

where a, the relative content of europium(II) in **1**, has been varied. The $\chi_M{}^{II}T$ contribution of the europium(II) ion, with its $4f^7\ {}^8S_0$ symmetric electronic ground state configuration, has been assumed to be independent of temperature and was constrained to be 7.877 emu K/mol, a value that corresponds

Table 4. Europium-151 Mössbauer Spectral Parameters[a] Obtained for $Na_{1.515}EuGeS_4$, 1

T (K)	δ (mm/s)[b]	eQ_gV_{zz} (mm/s)	eQ_gV_{zz} (MHz)	η	Γ (mm/s)	area (%)	area (%ε)(mm/s)	assignment
295	−12.13(6)	4.2(4)	73(7)	1	2.97	36.3(7)	11.0(2)	Eu(II)
	0.68(3)	2.2(3)	38(5)	1	2.97	63.7(7)	19.2(2)	Eu(III)
85	−11.79(6)	6.9(3)	120(5)	1	2.97	52.8(7)	26.3(3)	Eu(II)
	0.50(5)	4.8(3)	83(5)	1	2.97	47.2(7)	23.5(3)	Eu(III)

[a]Statistical fitting errors are given in parentheses. The actual errors are approximately twice as large. [b]The isomer shifts are given relative to 295 K EuF_3 powder.

dx.doi.org/10.1021/ic301724v | *Inorg. Chem.* 2012, 51, 11779−11786

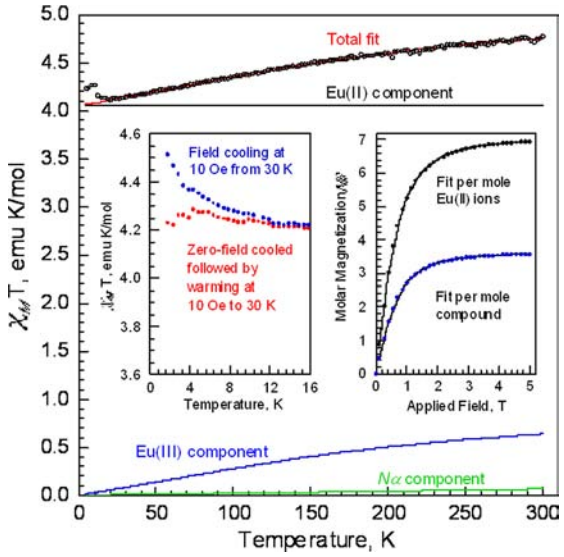

Figure 4. Temperature dependence of $\chi_M T$ of $Na_{1.515}EuGeS_4$, **1**, measured upon warming from 4.8 to 300 K in a 0.5 T dc applied magnetic field and fit between 20 and 300 K with a constant europium(II) contribution, in black, a europium(III) contribution calculated by using the Van Vleck expression, in blue, and a small second-order Zeeman contribution, $N\alpha T$, in green. The total fit, in red, passes through the data points and is mostly hidden. Left inset: the zero-field and field cooled $\chi_M T$ of **1** obtained in a 10 Oe applied magnetic field. Right inset: The magnetization of **1** measured at 1.8 K and fit with a $S = 7/2$ Brillouin function with $g = 2.003(3)$.

to an effective magnetic moment, μ_{eff}, of 7.937 μ_B for $S = 7/2$ and $g = 2$.

Although the europium(III) ion with its $4f^6\ ^7F_0$ $J = 0$ electronic ground state configuration might not be expected to contribute to the molar magnetic susceptibility, this is not the case as has been shown by Van Vleck.[30,31] This occurs because of the possible thermal population of the low lying $J > 0$ states associated with europium(III). Thus, the europium(III) contribution, $\chi_M{}^{III}T$, has been determined by using the expression derived by Van Vleck[30] and given as eq S6 of the SI. The details of this expression, which has also been used by other authors,[21,32] are discussed in the SI.

Finally, although the fit obtained with $N\alpha = 0$ in the above equation was adequate, see Figure S2 of the SI, it was found that the inclusion of $N\alpha = 0.00023(2)$ emu/mol significantly improved the fit of $\chi_M T$, especially above 200 K. This very small contribution to χ_M, see Figure S1 of the SI, may result from a combination of factors, such as a small error in the diamagnetic correction, a small Pauli paramagnetic contribution to the molar susceptibility, or a small second-order Zeeman contribution arising from the europium(II) ion; similar conclusions have been reported[21,32] earlier for some similar mixed valence europium compounds.

The fit of $\chi_M T$ and χ_M obtained between 20 and 300 K with the above components and with the $J = 0$, 1, and 2 terms in eq S6 of the SI is shown in Figures 4 and S1 of the SI. The resulting best fit parameters were $a = 0.515(5)$, corresponding to 51.5% of europium(II) and 48.5% of europium(III), a best stoichiometry of $Na_{1.515(5)}EuGeS_4$ for **1**, a splitting, E, between the ground $J = 0$ state and the first excited $J = 1$ state of 520(8) K or 360(6) cm^{-1}, and $N\alpha = 0.00023(2)$ emu/mol. A corresponding fit with only $J = 0$ and 1 was identical to the above fit within experimental error. Although there is a rather high correlation coefficient of 0.793 between the a and E fit parameters, a separate measurement of the magnetic susceptibility of the same preparation of **1** between 1.8 and 200 K led to a fit that was identical, within experimental error, with that given above, see Figure S3 of the SI. It should be noted that because of the very substantial contribution of the europium(II) and the small contribution of europium(III) at low temperatures, this analysis of $\chi_M T$ is the most accurate method for determining the best stoichiometry of **1**. Finally, it should be noted that, as expected, as the temperature approaches zero, the $\chi_M{}^{III}T$ contribution from the europium(III) ion approaches zero.

The $E = 360(6)$ cm^{-1} separation between the ground $J = 0$ state and the first excited $J = 1$ state of europium(III) agrees surprisingly well with the free-ion europium(III) value of 370 cm^{-1} reported[33] in the National Institute of Science and Technology table of energy levels for europium(III).

Because of the increase in $\chi_M T$ observed below ca. 15 K for **1**, see the main portion of Figure 4, its $\chi_M T$ was measured, after zero-field cooling, from 1.8 and 30 K in a 10 Oe applied field. This was followed by a field cooling study from 30 to 1.8 K. As may be seen in the left inset to Figure 4, below ca. 12 K the field cooled and zero-field cooled $\chi_M T$ results begin to diverge to a small extent, presumably as the result of the onset below ca. 12 K of long-range magnetic order. Alternatively, this divergence may be an indication of the presence of a trace of EuS, a europium(II) compound that is ferromagnetically ordered below a temperature that is variously reported[34−36] to be between 16 and 18 K. By using the approach described in the SI it has been estimated that the increase in χ_M and $\chi_M T$ of **1** observed below ca. 12 K would correspond to 0.08 to 0.18 wt % of EuS in the sample understudy. This amount of EuS would not be detected or be discernible by europium-151 Mössbauer spectroscopy, diffuse reflectance, or X-ray diffraction but, because of its large ferromagnetic susceptibility below the ordering temperature, EuS would be easily apparent in the magnetic studies. At this time it is difficult to determine whether the observed increase in χ_M and $\chi_M T$ below ca. 12 K is intrinsic to **1** or is the result of a trace of EuS impurity.

The critical Eu−Eu distance for ferromagnetic ordering through overlap of the 5*d* orbitals has been reported[36] to be 4.5 Å. In **1**, the Eu−Eu distances of 4.545 and 4.940 Å are larger than this critical distance. Hence, if **1** exhibits long-range ferromagnetic ordering, the ferromagnetic exchange must take place through superexchange pathways that involve the neighboring sulfur dianions.

The magnetization of **1** was measured at 1.8 K between 0 and 5 T. At 5 T **1** is close to saturation at 7 Nβ, see the right inset to Figure 4. A fit of the magnetization of **1** with a Brillouin function with $S = 7/2$ is virtually perfect and yields $g = 2.003(3)$, a value that agrees both with the expected g-value of 2 for europium(II) and the absence of any contribution from europium(III) at 1.8 K.

Optical Spectroscopy. The optical absorption characteristics of $Na_{1.515}EuGeS_4$, **1**, calculated from the diffuse reflectance spectrum by using the Kubelka−Munk function, are shown in Figure 5. The diffuse reflectance spectrum reveals the presence of both europium(II) and europium(III) and exhibits one broad absorption centered at 1.27 eV or 10,289 cm^{-1} and a sharp absorption edge at 1.45 eV, as well as several additional peaks arising from $4f$−$4f$ transitions of the europium(III) ion. The absorption at 1.27 eV and the absorption edge at 1.45 eV can be tentatively assigned to an

dx.doi.org/10.1021/ic301724v | Inorg. Chem. 2012, 51, 11779−11786

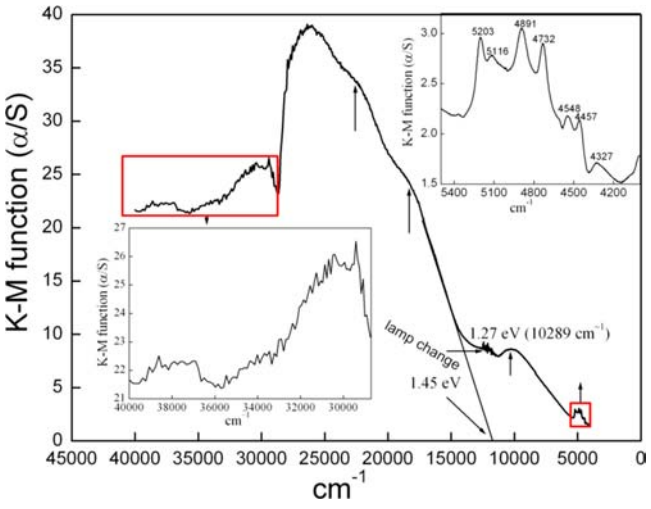

Figure 5. Optical absorption spectrum measured on crushed single crystals of $Na_{1.515}EuGeS_4$, **1**, transformed from the diffuse reflectance spectrum and shown as the Kubelka–Munk function α/S, the unitless ratio of the absorption coefficient to the scattering coefficient. The insets show an expanded view of the high and low energy portions of the spectrum.

intervalent charge transfer and a $4f-5d$ absorption arising from the europium(II) ion, respectively. A similar intervalent charge transfer absorption has been reported[37] in mixed valence Eu_3S_4. In addition to the broad absorption at 1.27 eV, additional bands observed between 4325 and 39 140 cm^{-1} are assigned to the following transitions based mainly on the previous work of Binnemans and Görller-Walrand.[38] Thus the absorptions between 36 900 and 39 140 cm^{-1}, see lower left inset to Figure 5, and between 28 900 and 32 090 cm^{-1} can be tentatively assigned to transitions to the crystal field split multiplet of ^3I_J and ^5H_J states starting from the degenerate $^7F_0$ ground state or the lowest excited manifold, $^7F_1$, i.e., the $^3I_J \leftarrow {}^7F_0$ or $^5H_J \leftarrow {}^7F_0/{}^7F_1$ transitions, respectively. The lower energy near-infrared bands, see upper right inset to Figure 5, can be assigned to the transitions to the crystal-field split states of the $^7F_6$ multiplet, originating from $^7F_1$ manifold as the $^7F_6 \leftarrow {}^7F_1$ transitions at 4457 and 4548 cm^{-1} and the nondegenerate $^7F_0$ state, as the $^7F_6 \leftarrow {}^7F_1$ transition between 4732 and 5203 cm^{-1}, respectively. The transition at 4327 cm^{-1} may be due to the $^7F_5 \leftarrow {}^7F_0$ or $^7F_5 \leftarrow {}^7F_1$ transition.

The remaining expected $4f-4f$ transitions, such as the $^5D_1 \leftarrow {}^7F_{0,1}$ transitions between 17 500 and 18 900 cm^{-1}, the $^5D_2 \leftarrow {}^7F_{0,1}$ transitions between 21 300 and 21 500 cm^{-1}, the $^5D_3 \leftarrow {}^7F_{0,1}$ transitions between 24 000 and 24 500 cm^{-1}, and the $^5L_6 \leftarrow {}^7F_{0,1}$ transitions between 24 500 and 26 000 cm^{-1} are buried in the absorption edge of the $4f-5d$ transition of the europium(II) ion and appear only as small inflections in the absorption edge. The transitions, such as the $^5D_0 \leftarrow {}^7F_0$ transition are completely masked by the $4f-5d$ transition of europium(II). It should be noted here that because neither the $^5D_1 \leftarrow {}^7F_1$ and $^5D_1 \leftarrow {}^7F_0$ transitions nor the $^5D_0 \leftarrow {}^7F_1$ and the $^5D_0 \leftarrow {}^7F_0$ transitions are well-resolved, it was not possible to derive the difference in energy between the $^7F_0$ ground state and the $^7F_1$ first excited state of europium(III) from the optical absorption spectra. For this reason, this energy difference was treated as a variable in the fit of the magnetic susceptibility of **1**, see Figure 4, and was found to be 360(6) cm^{-1}, a value that is in good agreement with the free-ion value[33] of 370 cm^{-1}.

CONCLUSIONS

In these studies, europium-151 Mössbauer and diffuse reflectance optical spectroscopy and magnetic susceptibility analysis conclusively confirm the europium ion mixed-valency in $Na_{1.515}EuGeS_4$, **1**. This mixed valency is a manifestation of the absence of sodium cations in the channels of **1**. In an earlier report[12] of the isostructural $Na_2EuSiSe_4$ compound, these channels were found to be filled with sodium cations and only europium(II) was present. The absence of any sodium cations in the channels of **1** could be due to the size of the channel, which is slightly smaller than that required by a sodium cation. If a hypothetical sodium cation is placed at the center of a perfect octahedron of six sulfur dianions in the channel, then the distance between the hypothetical sodium cation and the six sulfur dianions is 2.8161(3) Å, which is shorter than the average of 2.96(1) Å for the 12 Na–S distances found in **1**.

It should be noted that all attempts to synthesize Na_2EuGeS_4 in which the channels could be filled with sodium cations as in $Na_2EuSiSe_4$ failed. An attempted synthesis of the lithium-analogue of **1**, $Li_{1.515}EuGeS_4$, was also unsuccessful. However, by assuming that a smaller alkali cation, such as a lithium cation should fit into the channel, a mixed alkali system, $Na_{1.5}Li_{0.5}EuGeS_4$ is an important target for future synthetic work.

Another important difference between $Na_2EuSiSe_4$ and $Na_{1.515}EuGeS_4$, **1**, lies in their relative stabilities. $Na_2EuSiSe_4$ is very air-sensitive and decomposes quickly in air. In contrast, the as-synthesized long hexagonal rod shaped crystals of **1** are stable in air for as long as a year. However, a finely ground powder of **1** tends to oxidize after several months in air. Unfortunately, an attempt to exfoliate the nanotubules from a single crystal of **1** by simple sonication in DMF to yield uniform diameter inorganic nanotubes was unsuccessful.

Finally, it should be noted that $Na_{1.515(5)}EuGeS_4$, **1**, is yet another new composition of a rare nanotubular material that is self-assembled into a three-dimensional crystalline packing array. The channels of the empty tubules may, no doubt, be exploited for various oxidation–reduction based intercalation and selective host–guest chemistry. The isolation of uniform diameter nanotube compounds provides a future opportunity for studying their catalytic properties.

ASSOCIATED CONTENT

Supporting Information

A discussion of the Van Vleck equation and three additional magnetic susceptibility plots and X-ray crystallographic data in CIF format for **1**, $Na_{1.515}EuGeS_4$. This material is available free of charge via the Internet at http://pubs.acs.org.

AUTHOR INFORMATION

Corresponding Author

*E-mail: glong@mst.edu (G.J.L.); dorhout@ksu.edu (P.K.D.)

Present Address

[§]113 Eisenhower Hall, Kansas State University, Manhattan, KS 66506–1005, U.S.

Notes

The authors declare no competing financial interest.

ACKNOWLEDGMENTS

The authors thank Prof. Binnemans of the University of Leuven, Belgium, for helpful discussions regarding optical spectroscopy. The authors wish to acknowledge the financial

support provided by the National Science Foundation, NSF-DMR-0343412 and by the Fonds National de la Recherche Scientifique, Belgium, through Grant Nos. 9.456595 and 1.5.064.05.

REFERENCES

(1) Kamihara, Y.; Hiramatsu, H.; Hirano, M.; Kawamura, R.; Yanagi, H.; Kamiya, T.; Hosono, H. *J. Am. Chem. Soc.* **2006**, *128*, 10012. Takahashi, H.; Igawa, K.; Arii, K.; Kamihara, Y.; Hirano, M.; Hosono, H. *Nature* **2008**, *453*, 376. Kamihara, Y.; Hiramatsu, H.; Hirano, M.; Kawamura, R.; Yanagi, H.; Kamiya, T.; Hosono, H. *J. Am. Chem. Soc.* **2008**, *130*, 3296.
(2) Hsu, F.-C.; Luo, J.-Y.; Yeh, K.-W.; Chen, T.-K.; Huang, T.-W.; Wu, P. M.; Lee, Y.-C.; Huang, Y.-L.; Chu, Y.-Y.; Yan, D.-C.; Wu, M.-K. *Proc. Natl. Acad. Sci. U.S.A.* **2008**, *105*, 14262.
(3) Daage, M.; Chianelli, R. R. *J. Catal.* **1994**, *149*, 414. Raybaud, P.; Hafner, J.; Kresse, G.; Kasztelan, S.; Toulhoat, H. *J. Catal.* **2000**, *190*, 128. Merki, D.; Hu, X. *Energy Environ. Sci.* **2011**, *4*, 3878.
(4) Tenne, R.; Margulis, L.; Genut, M.; Hodes, G. *Nature* **1992**, *360*, 444. Tenne, R. *Nature Nanotechnol.* **2006**, *1*, 103.
(5) Rapoport, L.; Bilik, Yu.; Feldman, Y.; Homyonfer, M.; Cohen, S. R.; Tenne, R. *Nature* **1997**, *387*, 791. Rapoport, L.; Fleischer, N.; Tenne, R. *J. Mater. Chem.* **2005**, *15*, 1782.
(6) Albrecht-Schmitt, T. E. *Angew. Chem., Int. Ed.* **2005**, *44*, 4836.
(7) Millet, P.; Henry, J. Y.; Mila, F.; Galy, J. *J. Solid State Chem.* **1999**, *147*, 676.
(8) Krivovichev, S. V.; Kahlenberg, V.; Tananaev, I. G.; Kaindl, R.; Mersdorf, E.; Myasoedov, B. F. *J. Am. Chem. Soc.* **2005**, *127*, 1072.
(9) Krivovichev, S. V.; Kahlenberg, V.; Kaindl, R.; Mersdorf, E.; Tananaev, I. G.; Myasoedov, B. F. *Angew. Chem., Int. Ed.* **2005**, *44*, 1134.
(10) Adelani, P. O.; Albrecht-Schmitt, T. E. *Angew. Chem., Int. Ed.* **2010**, *49*, 1.
(11) Malliakas, C. D.; Kanatzidis, M. G. *J. Am. Chem. Soc.* **2006**, *128*, 6538.
(12) Choudhury, A.; Dorhout, P. K. *J. Am. Chem. Soc.* **2007**, *129*, 9270.
(13) Burns, P. C.; Kubatko, K.−A.; Sigmon, G.; Fryer, B. J.; Gagnon, J. E.; Antonio, M. R.; Soderholm, L. *Angew. Chem., Int. Ed.* **2005**, *44*, 2135. Forbes, T. Z.; McAlpin, J. G.; Murphy, R.; Burns, P. C. *Angew. Chem., Int. Ed.* **2008**, *47*, 2824. Sigmon, G. E.; Unruh, D. K.; Ling, J.; Weaver, B.; Ward, M.; Pressprich, L.; Simonetti, A.; Burns, P. C. *Angew. Chem., Int. Ed.* **2009**, *48*, 2737. Qiu, J.; Ling, J.; Sui, A.; Szymanowski, J. E. S.; Simonetti, A.; Burns, P. C. *J. Am. Chem. Soc.* **2012**, *134*, 1810.
(14) Bruker. *SMART*. Bruker AXS Inc., Madison, Wisconsin, U.S., 2002.
(15) Herrendorf, W. *HABITUS, A Program for the Optimization of the Crystal Shape for Numerical Absorption Correction*; University of Gießen: Gießen, Germany, 1995.
(16) Sheldrick, G. M. *Acta Crystallogr.* **2008**, *A64*, 112−122.
(17) Wendlandt, W. W.; Hecht, H. G. *Reflectance Spectroscopy*; Interscience Publishers: New York, 1966.
(18) Bain, G. A.; Berry, F. J. *J. Chem. Educ.* **2008**, *85*, 532.
(19) Robin, M.; Day, P. *Adv. Inorg. Chem. Radiochem.* **1968**, *10*, 247.
(20) Brown, I. D.; Altermott, D. *Acta Crystallogr.* **1985**, *B41*, 244.
(21) Wakeshima, M.; Doi, Y.; Hinatsu, Y.; Masaki, N. *J. Solid State Chem.* **2001**, *157*, 117.
(22) Cario, L.; Palvadeau, P.; Lafond, A.; Deudon, C.; Moelo, Y.; Corraze, B.; Meerschaut, A. *Chem. Mater.* **2003**, *15*, 943.
(23) Wu, Y.-D.; Naether, C.; Bensch, W. *Acta Crystallogr.* **2003**, *59E*, i137.
(24) Schleid, T.; Lauxmann, P.; Graf, C.; Bartsch, C.; Doert, T. *Z. Naturforsch.* **2009**, *64B*, 189.
(25) Grandjean, F.; Long, G. J. In *Mössbauer Spectroscopy Applied to Inorganic Chemistry*; Long, G. J., Grandjean, F., Eds.; Plenum Press: New York, 1989; Vol. 3, pp 513−597.
(26) Shenoy, G. K. In *Mössbauer Isomer Shifts*; Shenoy, G. K., Wagner, F. E., Eds.; North Holland: Amsterdam, 1978; p 102.
(27) Sauer, C.; Zaker, A. M.; Zinn, W. *J. Magn. Magn. Mater.* **1983**, *38*, 225. Wortmann, G.; Moser, J. *Hyperfine Interact.* **1981**, *10*, 879.
(28) Röhler, J.; Kaindl, G. *Solid State Commun.* **1981**, *37*, 737.
(29) Samuel, E. A.; Delgass, W. N. In *Mössbauer Effect Methodology*; Gruverman, I. J., Seidel, C. W., Eds.; Plenum Press: New York, 1976; Vol *10*, p 261.
(30) Van Vleck, J. H. *The Theory of Electric and Magnetic Susceptibilities*; Oxford University Press: London, 1944, pp 245−248.
(31) Van Vleck, J. H. *J. Appl. Phys.* **1968**, *39*, 365.
(32) Furuuchi, F.; Wakeshima, M.; Hinatsu, Y. *J. Solid State Chem.* **2004**, *177*, 3853.
(33) http://physics.nist.gov/cgi-bin/ASD/energy1.pl
(34) Teaney, D. T.; van der Hoeven, B. J. C., Jr.; Moruzzi, V. L. *Phys. Rev. Lett.* **1968**, *20*, 722.
(35) Shafer, M. W. *J. Appl. Phys.* **1965**, *36*, 1145.
(36) Mc Guire, T. R.; Argyle, B. E.; Shafer, M. W.; Smart, J. S. *Appl. Phys. Lett.* **1962**, *1*, 17.
(37) Allen, G. C.; Wood, M. B.; Dyke, J. *J. Inorg. Nucl. Chem.* **1973**, *35*, 2311.
(38) Görller-Walrand, C.; Huygen, E.; Binnemans, K. *J. Phys.: Condens. Matter* **1994**, *6*, 7797. Binnemans, K.; Görller-Walrand, C. *J. Phys.: Condens. Matter* **1996**, *8*, 1267. Binnemans, K.; Görller-Walrand, C. *J. Chem. Soc., Faraday Trans.* **1996**, *92*, 2487. Binnemans, K. *Bull. Soc. Chim. Belg.* **1996**, *105*, 793.